Click Here for Full Article

Hemispheric asymmetry of the magnetic field wrapping pattern in the Venusian magnetotail

T. L. Zhang,[1] W. Baumjohann,[1] J. Du,[1] R. Nakamura,[1] R. Jarvinen,[2] E. Kallio,[2] A. M. Du,[3] M. Balikhin,[4] J. G. Luhmann,[5] and C. T. Russell[6]

[1] We examine statistically the magnetic field in the Venusian magnetotail which is formed by the draping of interplanetary magnetic field lines. Although the near-planet and distant magnetotail regions have been sampled by the various missions to Venus and the general magnetic features of the distant magnetotail are well established, the near wake region from about 1.3 to 3 Venusian radii downstream of the planet remained unexplored until the Venus Express mission. Here we report the unanticipated finding of a draped field reversal in one hemisphere of the near Venus tail. When ordered by the interplanetary electric field orientation, the magnetic field lines in the hemisphere with inward motional electric field apparently are wrapped more tightly around Venus than in the other hemisphere, thus forming a field reversal region in the this portion of the near tail. A global hybrid simulation produces what we see and provides a three-dimensional view of the observed hemispherical asymmetry. **Citation:** Zhang, T. L., W. Baumjohann, J. Du, R. Nakamura, R. Jarvinen, E. Kallio, A. M. Du, M. Balikhin, J. G. Luhmann, and C. T. Russell (2010), Hemispheric asymmetry of the magnetic field wrapping pattern in the Venusian magnetotail, *Geophys. Res. Lett.*, *37*, L14202, doi:10.1029/2010GL044020.

1. Introduction

[2] Although there is no intrinsic magnetic field at Venus, it possesses a well-defined magnetotail [cf. *Phillips and McComas*, 1991]. Its tail arises through mass-loading of magnetic flux tubes carried by the solar wind, passing by the planet, and draping around the highly conducting ionosphere. Previous studies by PVO measurements reveal that the interplanetary magnetic field controls the general features of the Venus magnetotail [*Russell et al.*, 1981; *Saunders and Russell*, 1986; *McComas et al.*, 1986]. However, due to the PVO orbital geometry, our knowledge of Venus' tail is mainly from the distant tail region, 8 to 12 Venusian radii, R_V (= 6052 km) down the tail.

[3] For earth's magnetotail, it is well accepted that the near tail, 10–30 earth radii, R_E (= 6371 km) in the anti-solar direction, is the key region in harbouring various dynamic processes in understanding the magnetosphere as a whole [e.g., *Baumjohann*, 2002]. Since the Venus induced magnetosphere is much smaller, by a simple scaling factor of 10 to 1, the equivalent region at Venus will be 1–3 R_V down the tail. Venus Express, the first European mission to Venus, provides the first opportunity to access this key region and a detailed mapping of the average configuration is made possible [*Titov et al.*, 2006; *Svedhem et al.*, 2007]. Using more than three Venus years of data from the magnetometer on Venus Express, we perform a statistical study of the average structures of the near Venus magnetotail (in the range from 1 to 3 R_V down the tail). Here we report the first result of our ongoing undertaking on the near Venus magnetotail.

2. Magnetic Field Pattern in the Near Venus Magnetotail

[4] Figure 1 shows the spatial distribution of the magnetic field strength measured by the Venus Express magnetometer [*Zhang et al.*, 2006] during May 2006 and Dec 2008 in solar cylindrical coordinates. Here the 1-s resolution magnetic field data have been binned in 0.1×0.1 R_V bins. An induced magnetosphere [*Zhang et al.*, 2007] is evident with enhanced magnetic field enveloped around Venus with the magnetic barrier at the dayside and the extended magnetotail at the nightside. If we define the Venus magnetotail to be the induced magnetosphere region behind the planet, where the magnetic field is enhanced above magnetosheath levels, then it is apparent that the near Venus magnetotail has a radius about 1.3 R_V, not much larger than the optical shadow.

[5] Since the magnetic field of the tail arises from the convection of the solar wind field line against the planet, then one should be able to identify statistically the two lobes of the tail by rotating the magnetotail into a coordinate system ordered by the upstream magnetic field. *Russell et al.* [1981] report the first examination of field polarities in the distant Venus tail. They find the lobe structure with a separation of sunward and antisunward pointing lobe fields consistent with tail accretion from the solar wind. Figure 2 displays the cross-tail section of the field polarity distribution in the aberrated magnetic coordinate in which the X is anti-parallel to the solar wind flow, the Y axis is aligned with the cross-flow component of the interplanetary magnetic field, and the Z axis is aligned with the motional electric field, i.e., in the $-V \times B$ direction. In addition, the orbital motion of Venus is taken into account by considering the average aberration angle of 5°. Furthermore, unlike the Figure 1

[1]Space Research Institute, Austrian Academy of Sciences, Graz, Austria.
[2]Finnish Meteorological Institute, Helsinki, Finland.
[3]Institute of Geology and Geophysics, Chinese Academy of Sciences, Beijing, China.
[4]Department of Automatic Control and Systems Engineering, University of Sheffield, Sheffield, UK.
[5]Space Sciences Laboratory, University of California, Berkeley, California, USA.
[6]Institute of Geophysics and Planetary Physics, University of California, Los Angeles, USA.
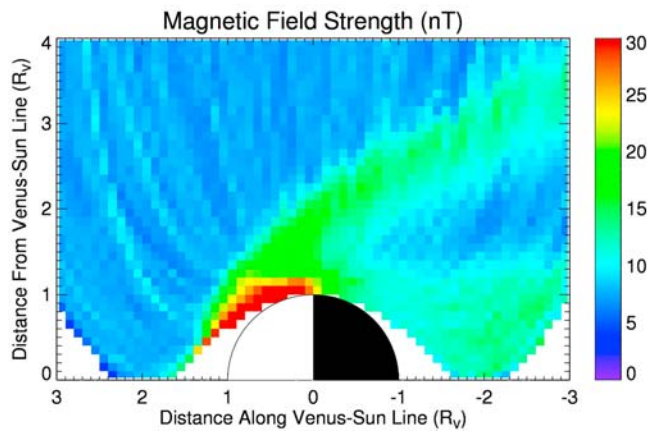
Figure 1. Distribution of the magnetic field strength around Venus observed by Venus Express magnetometer in 0.1×0.1 R_V bins.

Figure 3. Cross tail magnetic field component distribution. B_Y negative region in the −E hemisphere was not observed in the distant tail by PVO measurements.

which using data all Venus Express orbits in our studying interval, here we only select the orbits when the interplanetary magnetic field, IMF, is relative steady, defined by directional changes of the IMF between inbound and outbound of less than 30°. Altogether 358 orbits are selected to be rotated into magnetic coordinates. In constructing Figure 2, all field values within the tail (−1.2 R_V to −3.0 R_V in X range) are combined to determine the dominant polarity of the Bx field component within 0.2×0.2 bins in Y-Z plane. The view is toward the planet from the tail. The inner circle is the Venus optical shadow, and the outer dashed circle is the approximate size of the magnetotail with a radius about 1.3 Rv. It is evident in Figure 2 that the near Venus tail
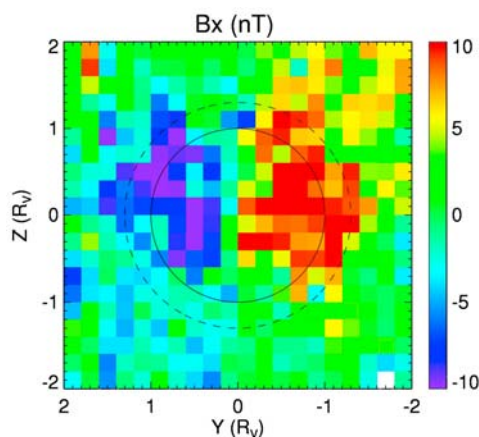
resembles the distant tail in magnetic polarity [*Saunders and Russell*, 1986].

[6] Our major result is displayed in Figure 3 showing the cross tail magnetic field B_Y distribution. While most of the tail has a cross tail field component B_Y in the positive Y direction expected for an induced magnetotail for the chosen direction the interplanetary magnetic field, there is clearly a negative B_Y region in the −E, i.e. −Z, hemisphere. While various motional electric field asymmetries have been revealed for Venus' bow shock, magnetosheath, distant tail structure etc [*Russell et al.*, 1988; *Zhang et al.*, 1991; *Saunders and Russell*, 1986], our finding of such a strong cross tail magnetic field asymmetry ordered by the electric field direction creating a negative B_Y region in the near tail is unanticipated.

[7] A simple explanation for this asymmetry is shown schematically in Figure 4. Our finding of negative B_Y in the −E hemisphere reveals that the two different draping patterns coexist and are controlled by the solar wind motional electric field. In the −E hemisphere, the magnetic field lines are more wrapped around the planet, suggesting convective flow penetrating deeper in which the magnetized plasma has reached lower altitudes. Finally, the reversal field pattern in the −E hemisphere may be enhanced by reconnection occurring in this hemisphere.

3. Global Hybrid Simulation of the Induced Magnetosphere

[8] We compare the observations to a global hybrid simulation, HYB-Venus, of the Venusian induced magnetosphere. In the model ions are treated self-consistently as particles moving in the electric and magnetic fields and electrons are modeled as a charge neutralizing fluid. The Venus version of the model is described by *Kallio et al.* [2006, 2008] and *Jarvinen et al.* [2009]. The Venus simulation run performed here has a spatial resolution of 0.1 R_V. The upstream parameters for the solar wind and the IMF are the nominal Venusian values: the solar wind speed, density, temperature and magnetic field are 430 km/s, 14 cm^{-3}, 10^5 K, (0, 5.88, 0) nT, respectively. Note that we consider a special IMF orientation ($B_X = 0$) to better illustrate the field draping.

Figure 2. Magnetic field polarity distribution in the near Venus magnetotail in magnetic coordinates in which the upstream IMF points in the Y direction. The view is toward the planet from the tail. The inner circle is the limb of Venus and the outer circle is the approximate magnetotail derived from Figure 1. The positive B_X values, i.e., fields pointing toward the sun, are found on the −Y side and the negative B_X values are found on the +Y side. This is as they should be for a solar wind origin.
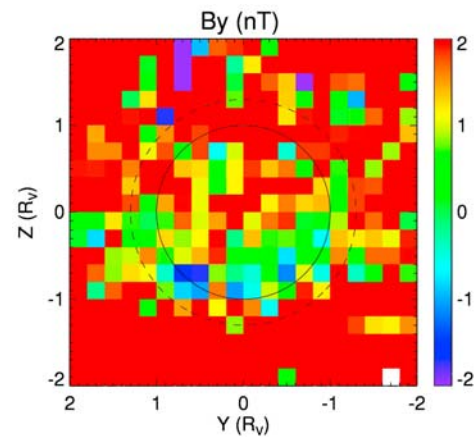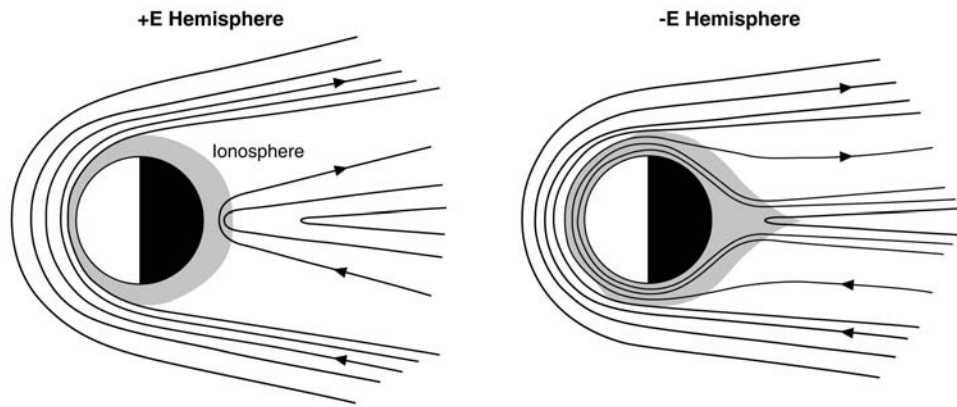
Figure 4. Schematic illustration of the field wrapping pattern in the two hemispheres (adopted from *Luhmann et al.* [1981], which originally depicted for the higher and lower solar wind dynamic cases) indicating that two different draping patterns coexist simultaneously.

The simulation coordinate system is defined as the same as in last section, i.e., the magnetic coordinates. See *Jarvinen et al.* [2009 and references therein] for more details about the Venus model.

[9] The calculated cross-tail magnetic field B_Y distribution at section $X = -1.2 \ R_V$ in the Y-Z plane is shown in Figure 5. As in the Venus Express observations, a negative B_Y region is clearly seen in the $-E$ hemisphere. In Figure 6, we display the magnetic field vectors in X-Y planes at $Z = +0.5 \ R_V$ and $-0.5 \ R_V$ respectively. Again, as in the Venus Express data, the simulation exhibits enhanced magnetic field line wrapping around the planet in the $-E$ hemisphere and a thin current sheet with a local field reversal in B_X occurs only in this hemisphere.

4. Conclusions

[10] The Venus Express orbital geometry has been excellent for studying the near Venus magnetotail at 1–3 R_V down the tail, a region devoid of coverage during the previous PVO observations. By sorting the magnetic field data in the interplanetary magnetic field coordinates, we reveal the hemispheric asymmetry of the field line draping pattern in the near tail at Venus. We find that the field line is more wrapped around Venus and forms a B_X reversal region in the $-E$ hemisphere than in the $+E$ hemisphere. Thus, the possible existence of magnetic x points in the low altitude wake has been observed by Venus Express in the $-E$ hemisphere of the near Venus tail.

[11] Our observations also suggest that the field lines in the $-E$ hemisphere are older than in the $+E$ hemisphere and by inference sink lower. In contrast, the field lines slip over the magnetic polar region more easily in the $+E$ hemisphere than that in the $-E$ hemisphere, and presumably the flow does not penetrate as deeply here. Then we would expect greater flux of atmospheric particles from the $+E$ hemisphere. Indeed, this is consistent with plasma observations from Venus Express [*Barabash et al.*, 2007] and Pioneer Venus [*Slavin et al.*, 1989].

[12] Finally, we apply a hybrid simulation to study the magnetic field draping patterns in three dimensions. Note that widely used ideal MHD models of planetary plasma interactions have symmetric $+E$ and $-E$ hemispheres if the input upper atmosphere depends only on the solar zenith angle as is usually the case. More general approaches such as Hall-MHD or hybrid simulations include kinetic effects capable of breaking this symmetry.

[13] The observed asymmetry suggests that the reconnection might occur preferentially in the $-E$ hemisphere. The reconnection process causes the field to cross the tail current sheet in the opposite direction to the direction of the IMF. If reconnection occurred, an isolated magnetic island might arise.
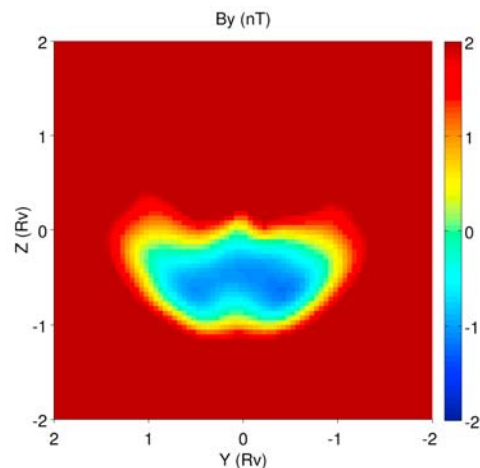

Figure 5. The magnetic field component B_Y distribution in Y-Z plane at $X = -1.2 \ R_V$ using the hybrid simulation described in the text.
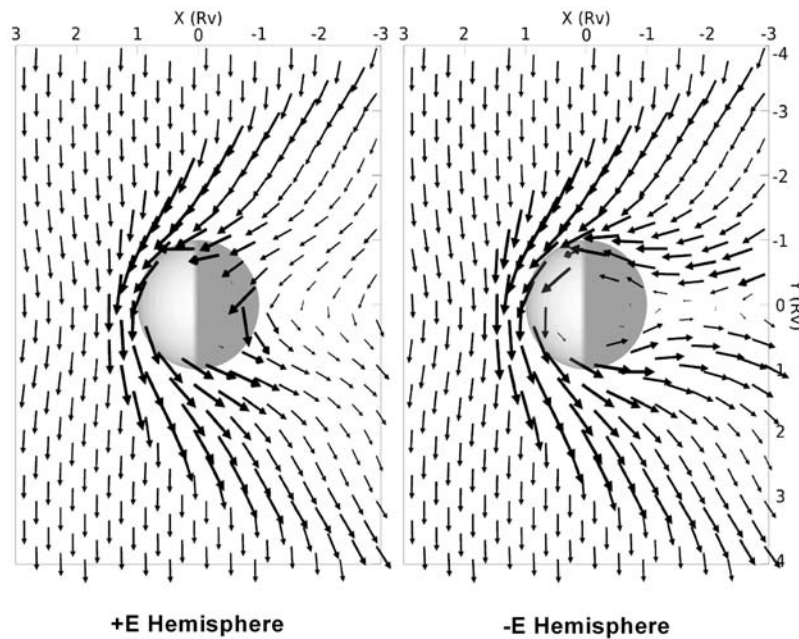
Figure 6. Average magnetic vectors calculated from hybrid simulation in X-Y for +E hemisphere (Z = 0.5 R$_V$ cut section) and −E hemisphere (Z = −0.5 R$_V$ section). The vector length indicates the field strength in nT, but with a upper limit of 10 nT.

References

Barabash, S., et al. (2007), The loss of ions from Venus through the plasma wake, *Nature*, *450*, 650–653, doi:10.1038/nature06434.

Baumjohann, W. (2002), Modes of convection in the magnetotail, *Phys. Plasmas*, *9*, 3665–3668, doi:10.1063/1.1499116.

Jarvinen, R., et al. (2009), Oxygen ion escape from Venus in a global hybrid simulation: role of the ionospheric O$^+$ ions, *Ann. Geophys.*, *27*, 4333–4348, doi:10.5194/angeo-27-4333-2009.

Kallio, E., R. Jarvinen, and P. Janhunen (2006), Venus-solar wind interaction: Asymmetries and the escape of O$^+$ ions, *Planet. Space Sci.*, *54*, 1472–1481, doi:10.1016/j.pss.2006.04.030.

Kallio, E., et al. (2008), The Venusian induced magnetosphere: A case study of plasma and magnetic field measurements on the Venus Express mission, *Planet. Space Sci.*, *56*, 796–801, doi:10.1016/j.pss.2007.09.011.

Luhmann, J. G. (1992), Pervasive large-scale magnetic fields in the Venus nightside ionosphere and their implications, *J. Geophys. Res.*, *97*, 6103–6121, doi:10.1029/92JE00514.

Luhmann, J. G., R. C. Elphic, C. T. Russell, J. A. Slavin, and J. D. Mihalov (1981), Observations of large scale steady magnetic fields in the nightside Venus ionosphere and near wake, *Geophys. Res. Lett.*, *8*, 517–520, doi:10.1029/GL008i005p00517.

McComas, D. J., H. E. Spence, C. T. Russell, and M. A. Saunders (1986), The average magnetic field draping and consistent plasma properties in the Venus magnetotail, *J. Geophys. Res.*, *91*, 7939–7953, doi:10.1029/JA091iA07p07939.

Phillips, J. L., and D. J. McComas (1991), The magnetosheath and magnetotail of Venus, *Space Sci. Rev.*, *55*, 1–80, doi:10.1007/BF00177135.

Russell, C. T., J. G. Luhmann, R. C. Elphic, and F. L. Scarf (1981), The distant bow shock and magnetotail of Venus: Magnetic field and plasma wave observations, *Geophys. Res. Lett.*, *8*, 843–846, doi:10.1029/GL008i007p00843.

Russell, C. T., E. Chou, J. G. Luhmann, P. Gazis, L. H. Brace, and W. R. Hoegy (1988), Solar and interplanetary control of the location of the Venus bow shock, *J. Geophys. Res.*, *93*, 5461–5469, doi:10.1029/JA093iA06p05461.

Saunders, M. A., and C. T. Russell (1986), Average dimension and magnetic structure of the distant Venus magnetotail, *J. Geophys. Res.*, *91*, 5589–5604, doi:10.1029/JA091iA05p05589.

Slavin, J. A., D. S. Intriligator, and E. J. Smith (1989), Pioneer Venus Orbiter magnetic field and plasma observations in the Venus magnetotail, *J. Geophys. Res.*, *94*, 2383–2398, doi:10.1029/JA094iA03p02383.

Svedhem, H., et al. (2007), The first European mission to Venus, *Planet. Space Sci.*, *55*, 1636–1652, doi:10.1016/j.pss.2007.01.013.

Titov, D. V., et al. (2006), Venus Express science planning, *Planet. Space Sci.*, *54*, 1279–1297, doi:10.1016/j.pss.2006.04.017.

Zhang, T. L., J. G. Luhmann, and C. T. Russell (1991), The magnetic barrier at Venus, *J. Geophys. Res.*, *96*, 11,145–11,153, doi:10.1029/91JA00088.

Zhang, T. L., et al. (2006), Magnetic field investigation of the Venus plasma environment: expected new results, *Planet. Space Sci.*, *54*, 1336–1343, doi:10.1016/j.pss.2006.04.018.

Zhang, T. L., et al. (2007), Little or no solar wind enters Venus' atmosphere at solar minimum, *Nature*, *450*, 654–656, doi:10.1038/nature06026.

W. Baumjohann, J. Du, R. Nakamura, and T. L. Zhang, Space Research Institute, Austrian Academy of Sciences, Schmiedlstr. 6, A-8042 Graz, Austria. (tielong.zhang@oeaw.ac.at)

R. Jarvinen and E. Kallio, Finnish Meteorological Institute, PO Box 503, FIN-00101 Helsinki, Finland.

A. M. Du, Institute of Geology and Geophysics, Chinese Academy of Sciences, No. 19, Beitucheng Xilu, Chaoyang District, 100029 Beijing, China.

M. Balikhin, Department of Automatic Control and Systems Engineering, University of Sheffield, Mappin Street, Sheffield S1 3JD, UK.

J. G. Luhmann, Space Sciences Laboratory, University of California, Berkeley, 7 Gauss Way, Berkeley, CA 94720-7450, USA.

C. T. Russell, Institute of Geophysics and Planetary Physics, University of California, Los Angeles, 3845 Slichter Hall, 603 Charles E. Young Dr., E, Los Angeles, CA 90065-1567, USA.